Journal of Neuropathology and Experimental Neurology

Vol. 58, No. 2
February, 1999
pp. 153–164

Experimental Investigation of Cerebral Contusion: Histopathological and Immunohistochemical Evaluation of Dynamic Cortical Deformation

DAVID I. SHREIBER, PHD, ALLISON C. BAIN, PHD, DOUGLAS T. ROSS, PHD, DOUGLAS H. SMITH, MD, T.A. GENNARELLI, MD, TRACY K. MCINTOSH, PHD, AND DAVID F. MEANEY, PHD

Abstract. We used a new approach, termed dynamic cortical deformation (DCD), to study the neuronal, vascular, and glial responses that occur in focal cerebral contusions. DCD produces experimental contusion by rapidly deforming the cerebral cortex with a transient, nonablative vacuum pulse of short duration (25 milliseconds) to mimic the circumstances of traumatic injury. A neuropathological evaluation was performed on brain tissue from adult rats sacrificed 3 days following induction of either moderate (4 psi, $n = 6$) or high (8 psi, $n = 6$) severity DCD. In all animals, DCD produced focal hemorrhagic lesions at the vacuum site without overt damage to other regions. Examination of histological sections showed localized gross tissue and neuronal loss in the cortex at the injury site, with the volume of cell loss dependent upon the mechanical loading ($p < 0.001$). Axonal pathology shown with neurofilament immunostaining (SMI-31 and SMI-32) was observed in the subcortical white matter inferior to the injury site and in the ipsilateral internal capsule. No axonal injury was observed in the contralateral hemisphere or in any remote regions. Glial fibrillary acidic protein (GFAP) immunostaining revealed widespread reactive astrocytosis surrounding the necrotic region in the ipsilateral cortex. This analysis confirms that rapid mechanical deformation of the cortex induces focal contusions in the absence of primary damage to remote areas 3 days following injury. Although it is suggested that massive release of neurotoxic substances from a contusion may cause damage throughout the brain, these data emphasize the importance of combined injury mechanisms, e.g. mechanical distortion and excitatory amino acid mediated damage, that underlie the complex pathology patterns observed in traumatic brain injury.

Key Words: Biomechanics; Brain injury; Cerebral contusion.

INTRODUCTION

Cerebral cortical contusions are among the most frequent clinical findings following traumatic brain injury (TBI) (1). Clinically, contusions are comprised, in part, of perivascular hemorrhages that appear as focal, wedge-shaped lesions involving the crowns of gyri (2–3). The leakage of blood cells, serum proteins, and neurochemicals due to cerebral contusions may induce secondary injury that include edema formation, uniform neuronal necrosis, and myelin degeneration within days to weeks after injury (4, 5).

All commonly used models of mechanically induced brain trauma in rodents designed to produce cortical contusion have also been found to induce damage to neurons and axons in regions physically separate from the contusion site (6). Accordingly, it has been widely accepted that focal brain injury may initiate a secondary injury cascade throughout the brain (7). This belief appears to be substantiated by the identification of a massive release of neurotoxic substances throughout the brain following trauma. In addition, therapeutic strategies designed to combat this secondary neurotoxicity have been shown to be highly neuroprotective in animal models of brain trauma (8). However, the role of cortical contusions in the secondary brain injury cascade following focal injury has not been elucidated. The biomechanics of common focal brain injury models, including fluid percussion, cortical impact, and weight drop, are often complex. As a result, determining the relative contribution of primary mechanical injury to the overall patterns of brain damage is difficult. Therefore, the mechanistic interactions between focal and diffuse damage in traumatic brain injury are not well understood.

The separate investigations of focal and diffuse traumatic brain injuries may clarify these interactions and, in turn, lead to more insight into the mechanisms and treatment of the more complex injury patterns observed clinically. As progress towards separating these injury patterns in experimental models, investigators have been successful in producing highly focal lesions in the rat brain by applying a rapid-onset, long-duration (5 s) vacuum pulse to the intact dura at the frontoparietal region in rats (9). Using this technique, investigators showed that nonhemorrhagic primary lesions could develop a delayed perivascular protein leakage and polymorphonuclear infiltration at the injury site (10). Moreover, this long duration vacuum pulse induced a prolonged reduction in blood flow at the site of injury, but did not cause ischemic cell damage. Remarkably, these occurred without overt hemorrhage at the lesion site, and point to the importance of changes that can occur from mild mechanical stress to the cortex.

From the Departments of Bioengineering (DIS, ACB, DFM) and Neurosurgery (DTR, DHS, TAG, TKM), University of Pennsylvania, Philadelphia, Pennsylvania.

Correspondence to: David F. Meaney, PhD, Department of Bioengineering, 3320 Smith Walk, University of Pennsylvania, Philadelphia, PA 19104–6392.

Sources of grant support: NIH PO1 NS-08803, NIH RO1 NS35712, NIH AG122527, and CDC R49/312712.

In the present study we used a model of traumatic brain injury, termed dynamic cortical deformation (DCD), to examine the relationship between focal hemorrhagic contusions and potential distal injuries to the brain. DCD uses a dynamic, nonablative, vacuum pressure to deform the exposed cortex and produce injury. The brief duration of the vacuum pulse (approximately 25 milliseconds) mimics the rapid tissue deformation that occurs during traumatic brain injury. In the present study, we identified the vascular, neuronal, and glial responses to 2 severities of DCD injury. We conducted this analysis to (1) examine the ability of DCD to produce focal lesions that are consistent with the clinical appearance of cortical contusions, and (2) examine whether focal hemorrhagic contusions can cause distal lesions that are not contiguous with the focal lesion at the site of deformation.

MATERIALS AND METHODS

Dynamic Cortical Deformation Device

Dynamic cortical deformation (DCD) produces lesions by applying a rapid, nonablative vacuum pulse to the exposed cortex (Fig. 1A). The injury is initiated by triggering the actuation of a solenoid valve, which is connected to a vacuum source. When the solenoid valve opens, a vacuum pressure pulse is applied to the brain through a specially designed aluminum couple via a Leur-Lok fitting. The dynamic vacuum pressure signal is measured by a pressure transducer (Entran, Fairfield, NJ), filtered and amplified, and sampled by a data acquisition system (Keithley/Metrabyte, Taunton, MA) in an IBM-compatible personal computer. The dynamic pressure trace is displayed on screen and recorded on disk for future analysis.

Surgery

Adult male, Sprague-Dawley rats (350–400 g, n = 18) were prepared for DCD in a manner similar to lateral fluid percussion as described previously (11). Two additional naive animals (anesthesia, no surgery) served as noninjured controls for the surgical procedure. Animals were anesthetized (sodium pentobarbital, 60 mg/kg, i.p.) and placed in a stereotaxic head holder on a thermostat-controlled heating pad to maintain core temperature. A 5-mm craniectomy was performed over the left parietal cortex. Under a dissecting microscope, the dura was removed in the region of the craniectomy, thus providing no mechanical resistance to the vacuum pulse. A Leur-Lock fitting was fixed to the craniectomy with a cyanoacrylate adhesive and secured with dental cement, resulting in an airtight seal with the mechanical couple. All surgical techniques were approved by the University of Pennsylvania's Institutional Animal Care and Use Committee.

Injury

Animals were divided into 3 groups (n = 6/group): 4 psi magnitude vacuum pressure (moderate severity DCD), 8 psi magnitude vacuum pressure (high severity DCD), and sham controls (surgery, but no injury). Injury severity relative to vacuum pressure was determined through a series of preliminary studies (n = 10) (unpublished observations). The index of DCD

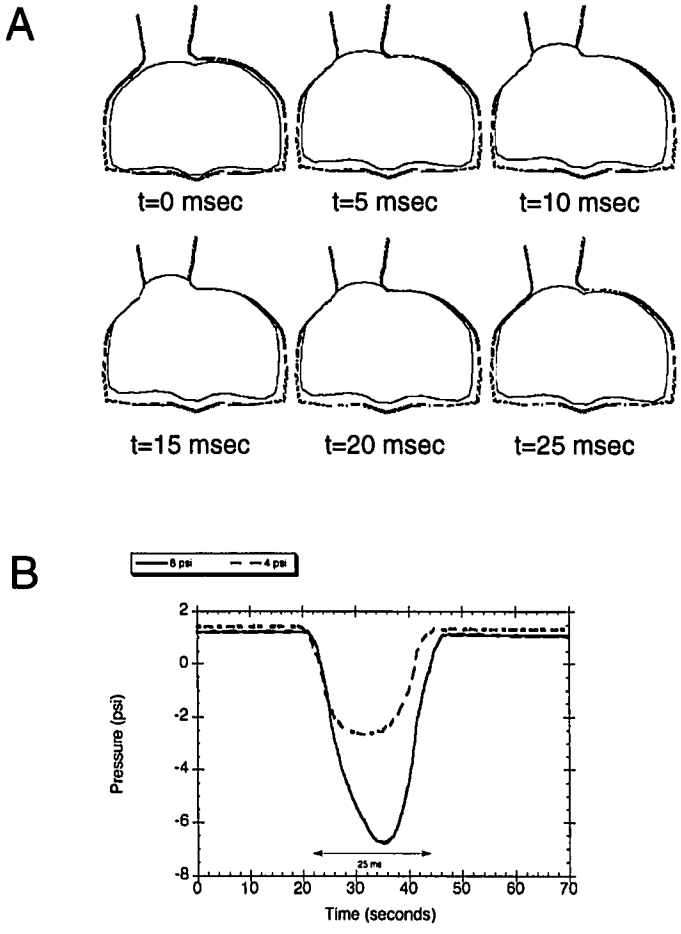

Fig. 1. (A) Overview of Dynamic Cortical Deformation technique. DCD induces injury by applying a dynamic vacuum pulse to the exposed cortex. The device allows independent control of the magnitude, duration, and shape of the vacuum pulse. The vacuum pressure is monitored by a vacuum pressure transducer and recorded with a data acquisition system. (B) Experimental pressure traces from DCD. In this study, 2 injury levels were used: moderate severity DCD (4 psi magnitude, dashed line) and high severity DCD (8 psi magnitude, solid line). The duration for both cases was 25 milliseconds.

severity (moderate vs high) was based on the modified contusion index for lateral controlled cortical impact (CCI) proposed by Goodman et al (12), to mimic the contusion index used in man (13, 3). To maintain fidelity to the dynamic nature of traumatic brain injury, a pulse duration of 25 milliseconds was selected for both the moderate and high severity (14, 15). An example trace of a vacuum pulse used in this study is shown in Figure 1B.

Gross Pathology and Histopathology

All animals were sacrificed 3 days postsurgery with a lethal dose of 6% chloral hydrate (10 ml/kg, i.m.) and perfused transcardially with heparinized saline, followed by 10% neutral buffered formalin, and finally 10% sucrose in buffered saline. Previous studies had demonstrated that a 3 day survival duration

was a sufficient time period to identify changes in axonal neurofilaments with the antibodies SMI-31 and SMI-32 (16, 17). The brains were stored in 30% sucrose-saline for cryoprotection during processing. Two brains from each group were sectioned coronally into 1-mm sections and photographed for gross observation of cerebral hemorrhage. The remainder of the brains (n = 4/group) were cut coronally around the injury site into ~2 cm blocks, sliced on a sliding microtome into 40-μm-frozen sections, and catalogued in 6 serial sets. Two sets were mounted and stained with cresyl violet (Nissl stain) or hematoxylin and eosin (H&E). Other sets were reacted for immunohistochemistry and visualized using the avidin-biotin peroxidase method (Vector Labs, Ingold, CA). One set was saved for future analysis. Additionally, the cerebellum and lower brainstem from 2 brains in each group were cut sagittally into 40-μm sections and stained to inspect for damage remote from the injury site.

Axonal injury was assessed immunohistochemically using the following mouse monoclonal antibodies at 1:10,000 dilution (Sternberger and Meyer Monoclonals, Inc., Baltimore, MD): SMI-31 to recognize epitopes to the phosphorylated medium and heavy weight neurofilament proteins, and SMI-32 to recognize epitopes common to nonphosphorylated heavy and medium weight neurofilament proteins. Astrocytic reactivity was examined with a polyclonal glial fibrillary acidic protein antibody (GFAP) (gift from Dr. Larry Eng). Preliminary immunostaining for axonal changes demonstrated intense background staining of endogenous rat immunoglobulins due to the hemorrhagic nature of the lesions. To remedy this, the secondary antibody used for detection of axonal pathology (SMI-31, SMI-32) was thoroughly adsorbed by a solid-phase technique to remove antibodies that cross-react with rat immunoglobulins (biotinylated horse anti-mouse IgG rat adsorbed, Vector Laboratories). In comparison, preadsorption for rat IgG with GFAP was not necessary due to lower background staining, and a secondary antibody (biotinylated goat anti-rabbit IgG, Vector Laboratories) was used directly to detect astrocytic reactivity. Also, a small amount of crystalline bovine serum albumin was added to decrease nonspecific binding during incubation in both monoclonal and polyclonal primary antibodies.

Analysis

The severity of the injury was graded by calculating the volume of tissue demonstrating necrosis or neuronal loss. Macroscopic grayscale images of H&E sections were captured with an image acquisition system (AIS Image LC, St. Catherines, Ontario). Lesioned areas were traced using the contralateral cortex as a control to establish pixel density thresholds for injury. To account for swelling or other tissue distortions, the image of the lesioned area image was subtracted from the ipsilateral hemisphere. The remainder of the ipsilateral hemisphere was mirrored on to and subtracted from the contralateral hemisphere. The remaining image was considered the corrected lesion area. The corrected lesion area was calculated for alternate sections, summed, and multiplied by the linear distance between measured slices (480 μm) to arrive at a lesion volume. Lesion volume was analyzed with an orthogonally designed ANOVA; $p < 0.05$ was considered statistically significant.

RESULTS

General Neuropathology

Sham Group: The findings from the sham group were consistent with the neuropathology associated with removal of the dura (18). Histology and immunohistochemistry of the sham surgery animals revealed subtle, superficial pathology in 2 of the 4 animals when compared to naive animals, including distortion and cell loss in the superficial layers of the cortex at the surgery site in association with limited reactive astrocytosis (Fig. 2). In the remaining 2 animals, astrocytic activity and cell loss were less marked.

Moderate Severity DCD Injury: All animals exposed to a 4-psi, 25-millisecond vacuum demonstrated focal petechial hemorrhage at the cortical injury site. Overt hemorrhage extended through layers III and IV of the cortex in all animals (Fig. 3). Small hemorrhages were observed at the gray/white matter junction immediately inferior to the injury site. No other gross lesions were observed. Cresyl violet and H&E histology demonstrated necrotic tissue and extensive cell body loss in the cortex below the injury site, which extended through layer V of the cortex for one animal and through layer VI to the gray/white matter junction for the other 3 cases (Fig. 4). Eosinophilic changes and nuclear pyknosis were observed in neurons adjacent to the necrotic region. No cellular loss was observed in areas traditionally injured in other models of experimental brain injury, including the ipsilateral and contralateral CA_3 subfield and dentate hilus of the hippocampus, substantia nigra, and basal ganglia. No abnormalities were observed in the lower brainstem and cerebellum. SMI-31 and SMI-32 immunohistology identified axonal damage in the form of axonal terminal bulbs concentrated in the subcortical white matter immediately inferior to the injury site, and axonal pathology in the ipsilateral internal capsule (Fig. 5). GFAP immunohistology detected reactive astrocytes throughout the ipsilateral cortex (Fig. 5). Astrocytic hypertrophy was also found outside the regions of neuronal loss in the ipsilateral cortex.

High Severity DCD Injury: In the 8 psi, 25-millisecond group, gross hemorrhage was observed at the injury site and extended through the cortex and subcortical white matter to the hippocampus in all animals (Fig. 6). Cresyl violet and H&E staining demonstrated necrotic tissue and cell body loss that surrounded the necrotic cavity (Fig. 7). A consistent cell loss and distension of the ipsilateral hippocampal structure was observed in all animals; the margin of cellular loss ranged from the CA_1 subfield of the hippocampus (n = 2 animals) to the polymorph layer of the dentate gyrus (n = 2 animals). In cases with cell loss in the dentate gyrus, the cellular loss included complete loss of the pyramidal cell layer of the CA_1 subfield and minor loss in the polymorph layer of the dentate

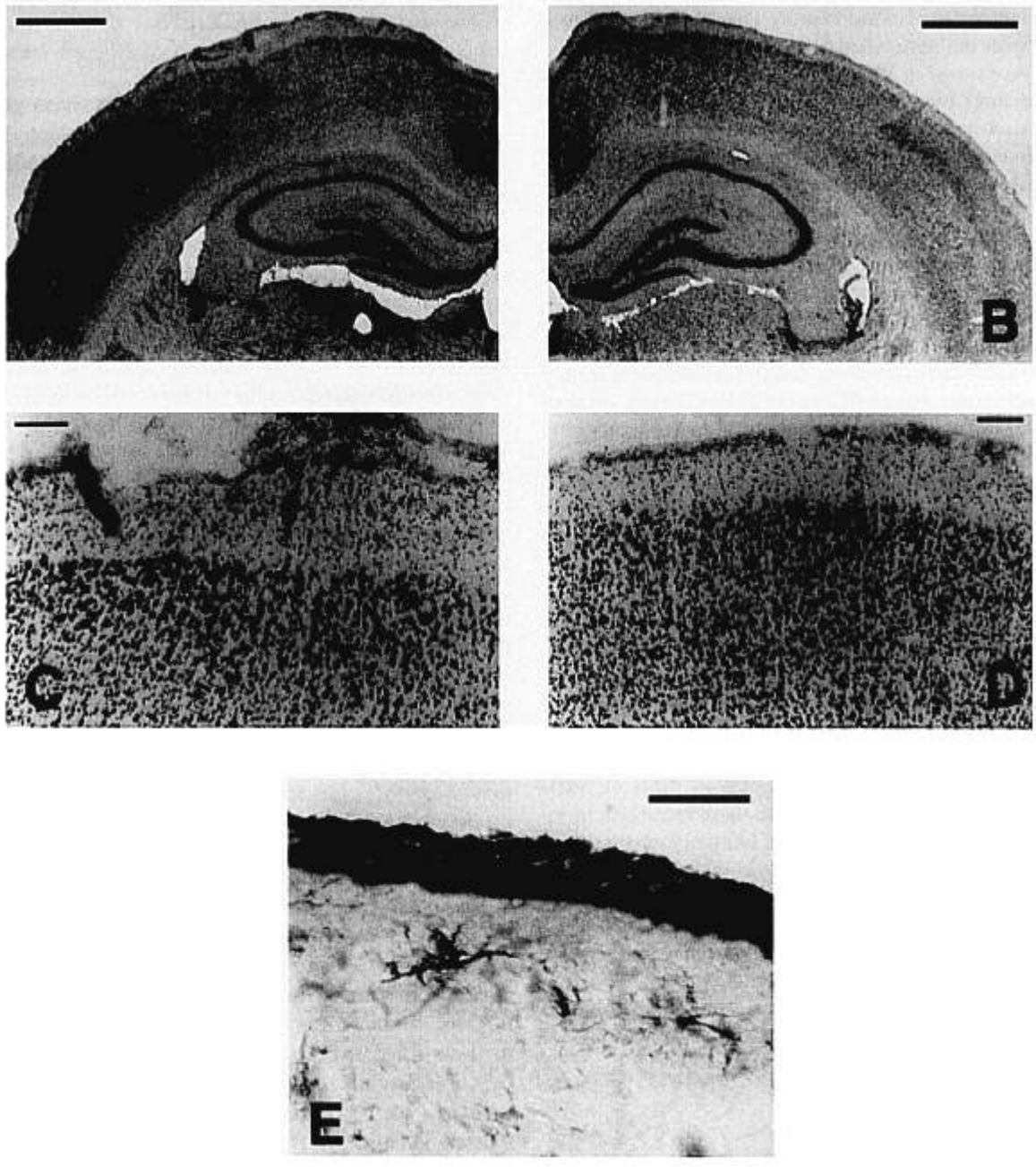

Fig. 2. Evaluation of surgical procedure. Cresyl violet staining following the surgical procedure demonstrated that removal of the dura caused some distortion and subtle pathology in the ipsilateral cortex (A, C) when compared to the contralateral side (B, D). (E) Photomicrograph of astrocytic reactivity (GFAP) after sham surgery. The mild gliosis at the surgery site was consistent with morphology following a breach of the dura. Bars: (A, B): 1 mm. (C, D): 100 μm. (E): 50 μm.

gyrus, where perivascular hemorrhage was observed. However, no gross cellular loss was observed in areas not contiguous with the primary lesion, including the CA_3 subfield of the hippocampus, the brainstem, and the cerebellum. SMI-31 and SMI-32 immunohistochemistry identified axonal swellings and bulbs in the subcortical white matter immediately below the injury site (Fig. 8). Axonal fragmentation was found more laterally throughout the ipsilateral internal capsule. The boundaries and numbers of axonal bulbs were qualitatively greater for the high severity group than for the moderate severity group. GFAP immunohistology detected reactive astrocytes surrounding the necrotic region (Figure 8).

The degree of astrocytosis was qualitatively most pronounced directly inferior to the injury site. Reactive astrocytes were found outside the regions of neuronal loss identified by cresyl violet for slices at the same anatomical level.

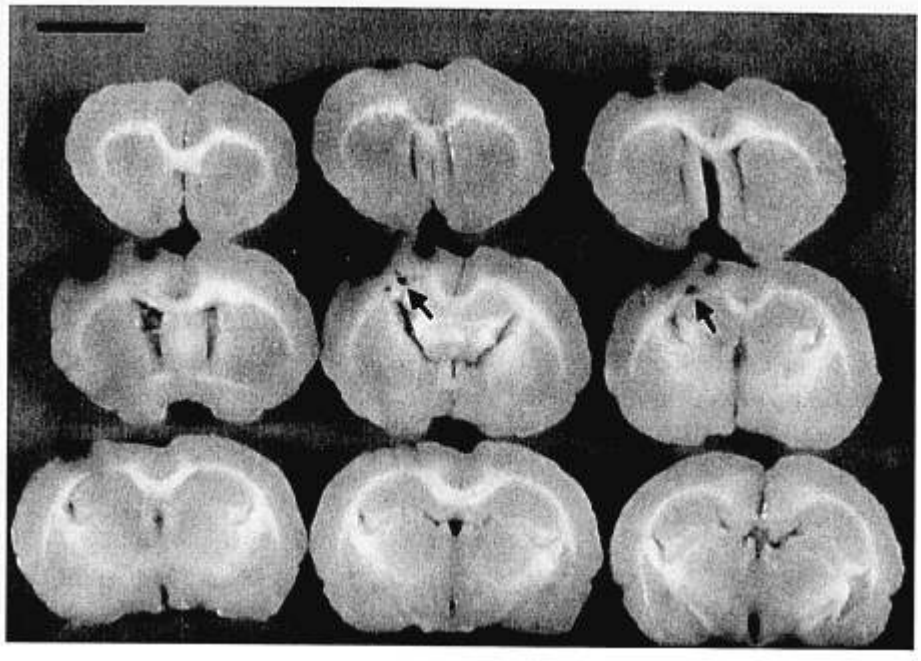

Fig. 3. Gross (1-mm-thick) coronal sections of brain exposed to moderate severity DCD. The hemorrhagic lesion shape ranged from hemispherical to wedge-shaped and extended through layers III and IV of the cortex. Some parenchymal lesions were observed at the gray/white matter junction (arrows). No overt hemorrhage was observed in regions remote from the injury site. Bar: 1 cm.

Lesion Volume

Statistical analysis of the lesion volume data (Fig. 9A, B) for the 3 injury groups revealed significant differences among the means of injured groups vs uninjured groups (ANOVA, $p < 0.001$). Furthermore, a significant difference existed between the lesion volume of the high severity DCD and moderate severity DCD groups (ANOVA, $p < 0.001$).

DISCUSSION

We report that hemorrhagic contusions of a controllable size were produced by dynamic cortical deformation. The applied deformation produced not only a well-circumscribed hemorrhagic lesion, but also graded cell loss, extensive gliosis, and axonal damage in areas immediately adjacent to the lesion cavity. Moreover, the wedge-shaped contusions observed in this study closely represent the geometry of lesions observed in human head injury (1). Unlike most rodent models of brain trauma, where cortical contusions are found in association with widespread damage, the damage from dynamic cortical deformation was confined to only the region immediately surrounding the applied mechanical loading. Astrocytic hypertrophy was the most extensive lesion examined and was confined to the ipsilateral hemisphere, contiguous with the zone of neuronal loss. No damage was observed in other areas. It is worth noting that localized cortical damage can also be produced using other techniques such as freezing (18), and ablation (19). However, the ability to produce a graded, localized lesion with the DCD method allows one to examine a range of lesion sizes in the cortex. From these observations, we conclude that dynamic cortical deformation is uniquely suitable for examining the consequences of cerebral contusions in isolation from other brain injuries.

Traumatic injury often involves a complex combination of primary tissue damage, breakdown of the blood-brain barrier, and changes due to secondary injury phenomena. The relationships among localized tissue deformation, hemorrhage, and widespread injury patterns in the brain are not fully understood. However, to elucidate these relationships, it is useful to examine separately the factors that could contribute to different patterns of damage in the brain following trauma. For instance, it has been shown that a transient change in intracranial pressure coupled with the release of blood-borne constituents into the interstitial space can cause focal lesions in the cortex, creating areas of necrosis that may encompass up to 15% of the injured hemisphere (20). In contrast, the presence of only an autologous blood clot on the brain surface causes no significant cell loss or necrosis in cortical and/or subcortical structures (21).

In models such as lateral fluid percussion, cortical impact, and weight drop, it is often suggested that cortical contusions may initiate the secondary damage observed in selectively vulnerable regions remote from the focus of injury, such as the hippocampus, thalamus, and septum. Our

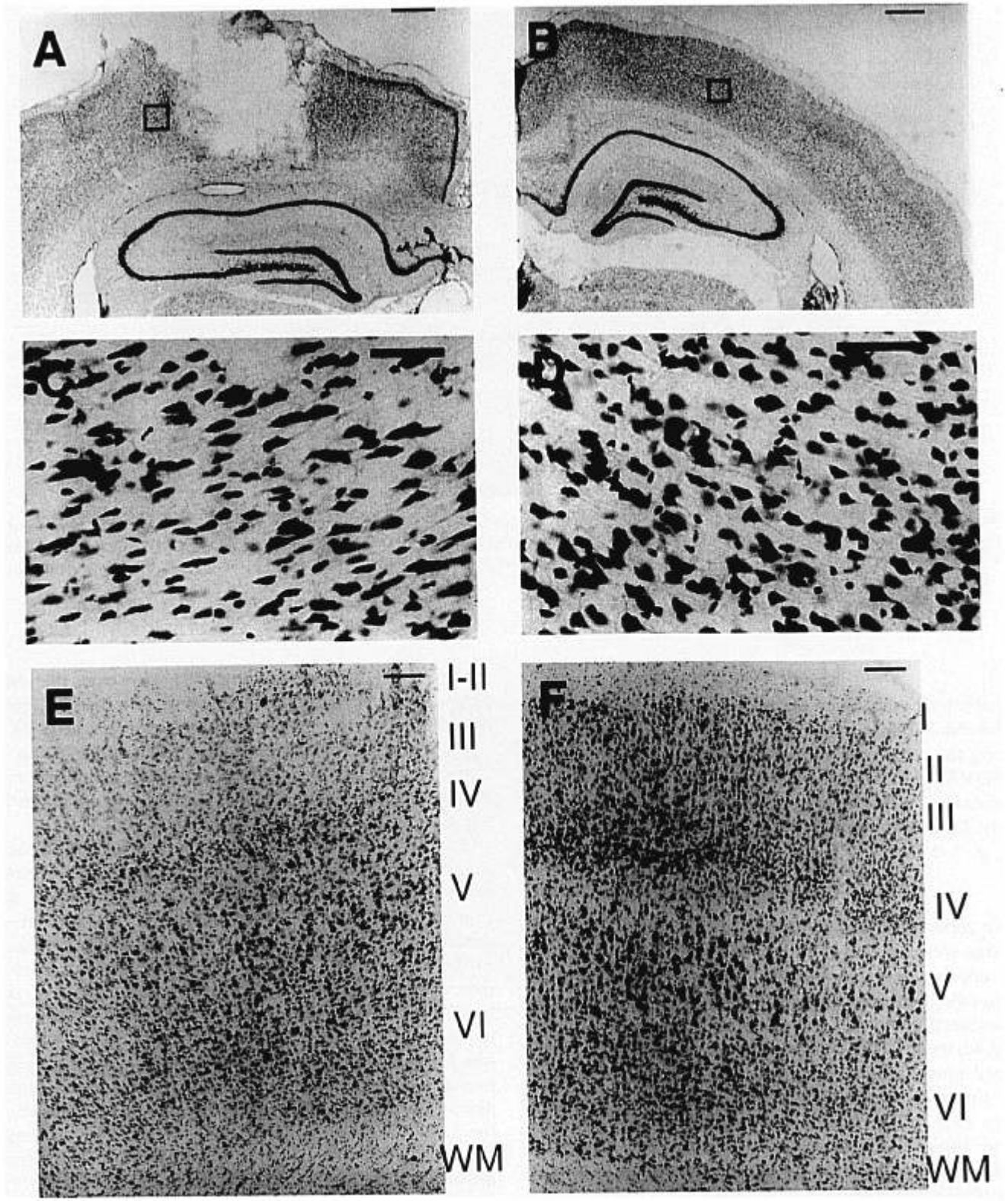

Fig. 4. Photomicrographs of cresyl violet stained sections after moderate severity DCD. (A) A necrotic cavity extends to the gray/white matter junction in the cortex ipsilateral to injury. The hippocampus and other remote regions appeared uninjured. (B) No pathology was observed in the contralateral cortex. Boxed regions in (A) and (B) are shown in (C) and (D), respectively. (C) Irregular, elongated cell bodies were found adjacent to the necrotic cavity, whereas regularly shaped cell bodies were observed in the contralateral cortex (D). (E) Slightly rostral to the main coronal axis of the injury, the necrotic cavity is not as advanced, but a general disruption of the cortical layers is observed. Layers I–III demonstrate a marked decrease in cellularity and some necrosis. The decrease in Nissl stain continues through Layer V. Layers VI and the white matter (WM) appear normal. (F) Contralateral cortex shows no significant changes. Bars: (A, B): 500 μm; (C, D): 50 μm; (E, F): 100 μm.

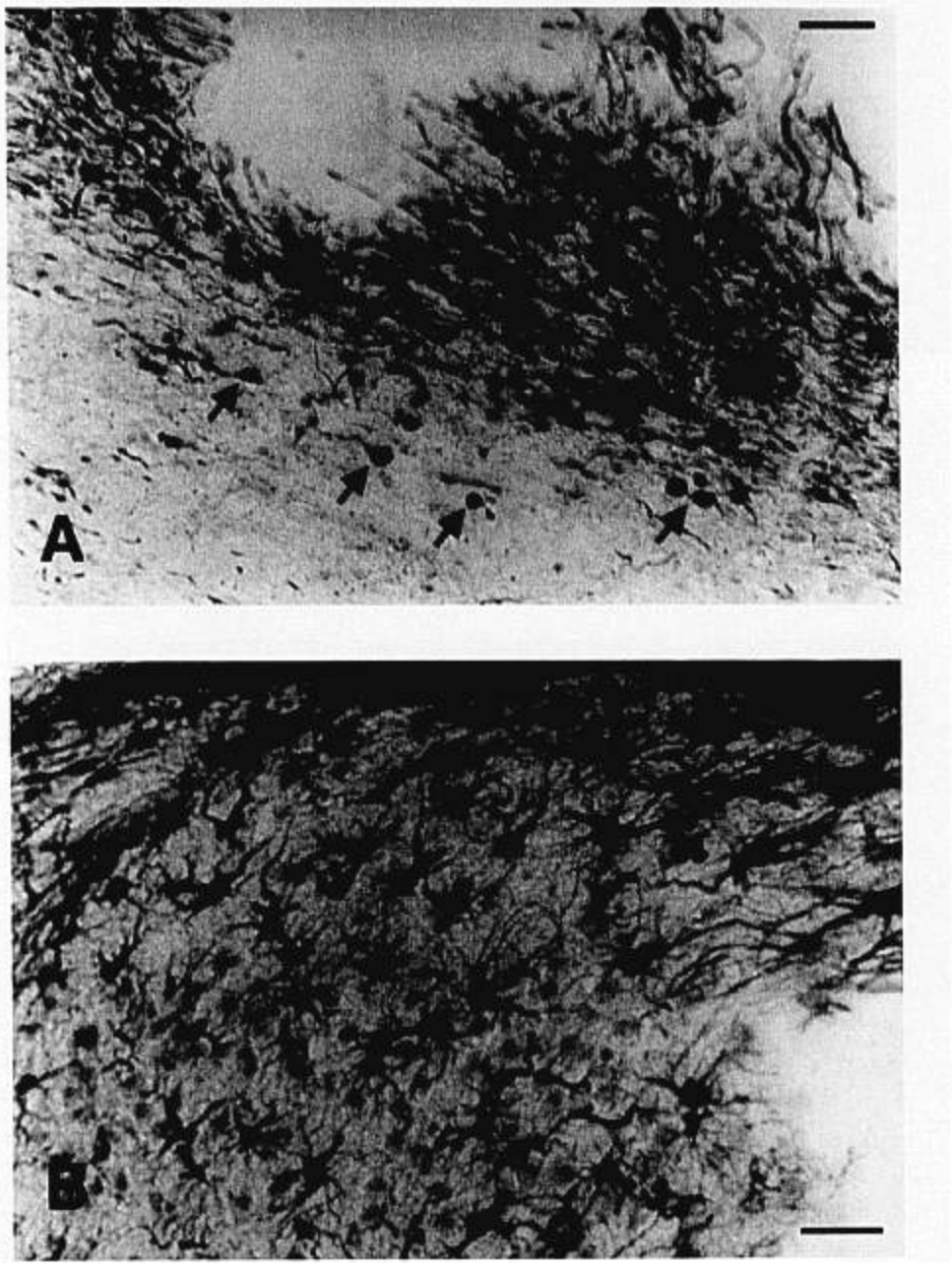

Fig. 5. Immunohistochemistry following moderate severity DCD. (A) High power photomicrograph of nonphosphorylated neurofilament protein (SMI 32) immunostained section from moderate severity DCD. Terminal clubbing is apparent in the subcortical white matter directly inferior to the injury site (arrows). No terminal clubbing was observed in regions remote from the injury, including the contralateral hemisphere, midbrain, basal ganglia, and cerebellum. (B) Photomicrograph of astrocytic reactivity (GFAP) for moderate severity DCD lateral to the necrotic cavity. Astrocytic reactivity was concentrated around the injury site in the ipsilateral cortex. Bars: 25 μm.

investigation shows that, 3 days following injury, the combination of mechanical tissue deformation and the release of blood-borne substances into the extracellular space does not create significant injury in areas remote from the site of primary cell loss and necrosis. Interestingly, a very focal deformation at the moderate injury level is unable to produce damage in nearby ipsilateral structures such as the CA3 subfield of the hippocampus and the dentate hilus, even with the presence of blood-borne substances, such as excitatory amino acids, in the interstitial space. At higher levels, cell loss in ipsilateral subfields of the hippocampus such as CA1 provide a common link with hippocampal pathology observed in human traumatic brain injury (22), yet the cell loss regions were always contiguous with the necrotic zone and never extended into the contralateral hippocampus. Therefore, our results do not support the link

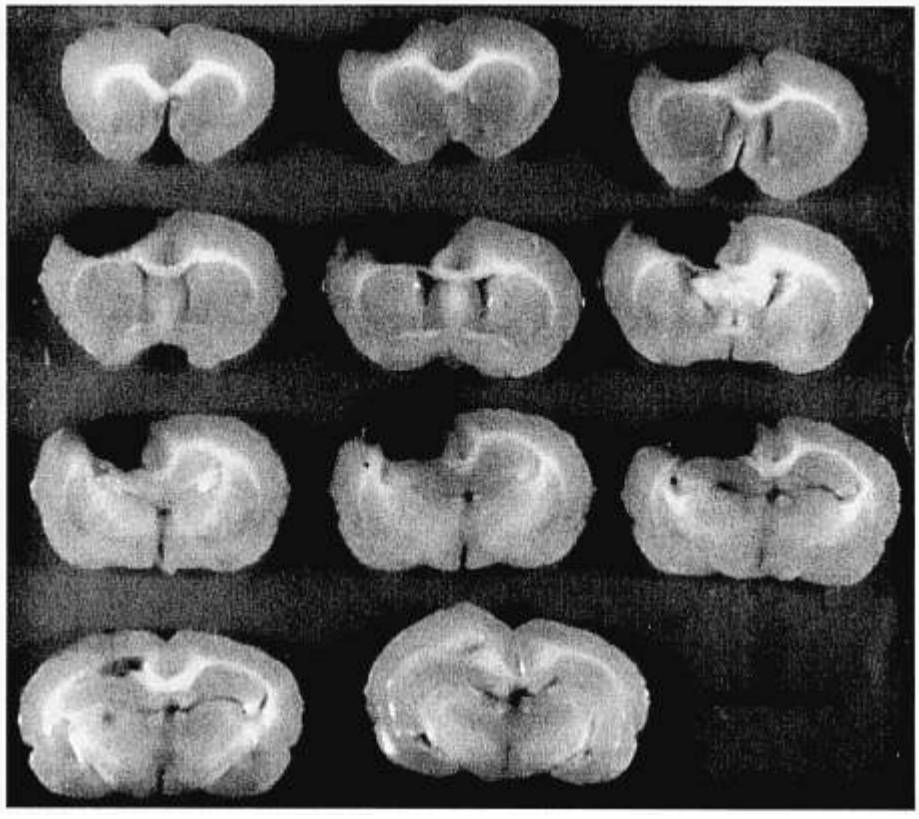

Fig. 6. Gross (1-mm-thick) sections of brain exposed to high severity DCD. The hemorrhagic contusion extended through the cortex and subcortical white matter to the CA_1 subfield of the hippocampus. No overt hemorrhage was observed in regions remote from the injury site. Bar: 1 cm.

between a cortical contusion and widespread histopathological damage. While our finding showing the absence of damage remote from the focal contusion site by 3 days postinjury is unique to other brain trauma models, the possible appearance of temporally delayed damage or scattered cell loss detected with cell counting techniques cannot be discounted.

While alternative explanations for widespread damage include ischemia and abnormal neurochemical levels, we believe the primary reason we see dramatically different neuropathological outcomes between DCD and percussion or direct impact models of focal brain injury are the differences in the injury biomechanics amongst these techniques. For most small animal models of traumatic brain injury, injury is induced by a focal compression of the cortex. Due to the incompressible mechanical behavior of brain tissue and the geometry of the skull, focal compression leads to both local and remote variations in the intracerebral strain field (23–25). This complicated strain field can cause tissue deformation and injury in areas that are distal to the site of percussion or impact. For DCD, the deformation experienced by the brain is restricted to the region contiguous with the applied load (26). Deformation of tissue in widespread regions is not observed in a biomechanical analysis of DCD, and therefore provides a direct explanation for the highly localized injury pattern observed in this model.

The modulation of intracerebral strains by the presence or absence of the dura is the likely reason for the differences observed in our model and another model of focal brain injury, termed suction impact, that was reported recently (9, 10, 27). In suction impact, a vacuum pulse applied to the exposed dura results in a localized increase in microvascular permeability, a regional reduction in cerebral blood flow, and subsequent delayed edema, but no overt hemorrhage. We believe that the difference in surgical preparation between suction impact and DCD produces different biomechanical loading conditions at the moment of injury. In DCD, we retract the dura and expose directly the arachnoid surface to the vacuum pulse. The mechanical properties of the dura are significantly stiffer than brain tissue (28), and thus larger pressures are required to deform the cortex when the dura is left intact. Therefore, at identical pressure levels, DCD will produce more extensive damage than suction impact. Together, these 2 techniques now offer an opportunity to study the mechanisms and therapeutic strategies for a continuum of contusions, ranging from subtle ultrastructural changes to an immediate opening of the blood brain barrier.

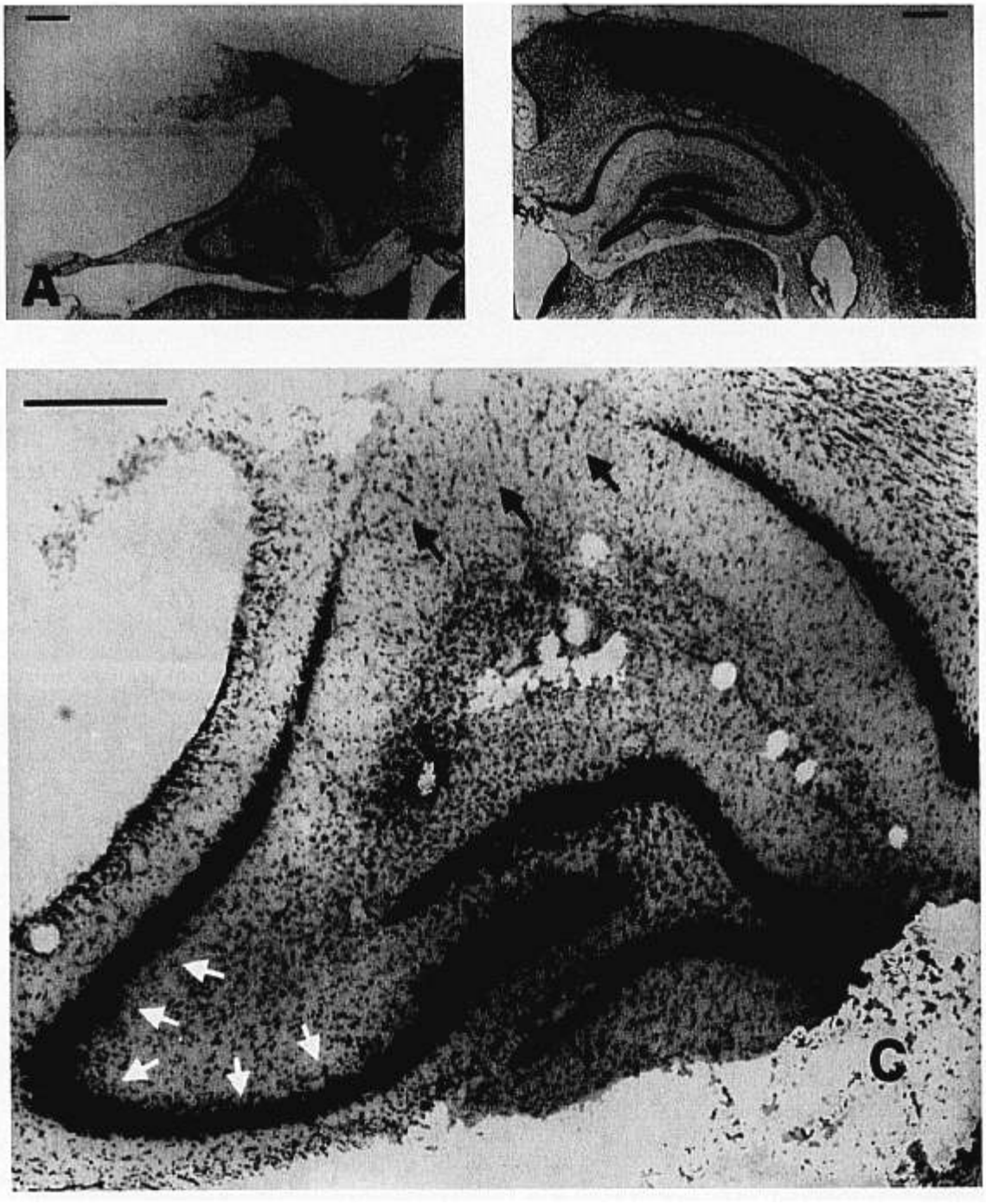

Fig. 7. Photomicrographs of cresyl violet stained sections following high severity DCD. (A) An advanced necrotic cavity was observed ipsilateral to the injury site and extended through the full cortical thickness and subcortical white matter into the hippocampus. (B) The contralateral cortex appears uninjured. (C) Ipsilateral hippocampus 480-μm caudal to (A) and (B). When viewed at higher magnification, the ipsilateral hippocampus demonstrates complete loss of the CA1 subfield (black arrows), hemorrhage of vessels in the hippocampus, and minor loss in the polymorph layer of the dentate gyrus. However, no pathology is observed in the CA3 subfield (white arrows). Bars: 500 μm (A, B): 500 μm.; (C): 100 μm (C).

The absence of widespread damage following DCD may have important consequences on the therapeutic strategies after traumatic brain injury. For instance, following acute injury in humans, it is now well established that levels of excitatory amino acids, such as glutamate, increase significantly in the cerebrospinal fluid to levels that can injure neurons in culture (29–31), raising the possibility of widespread in vivo neuronal damage due to excitoxicity. However, recent data show that these elevated levels of glutamate in the cerebrospinal fluid do

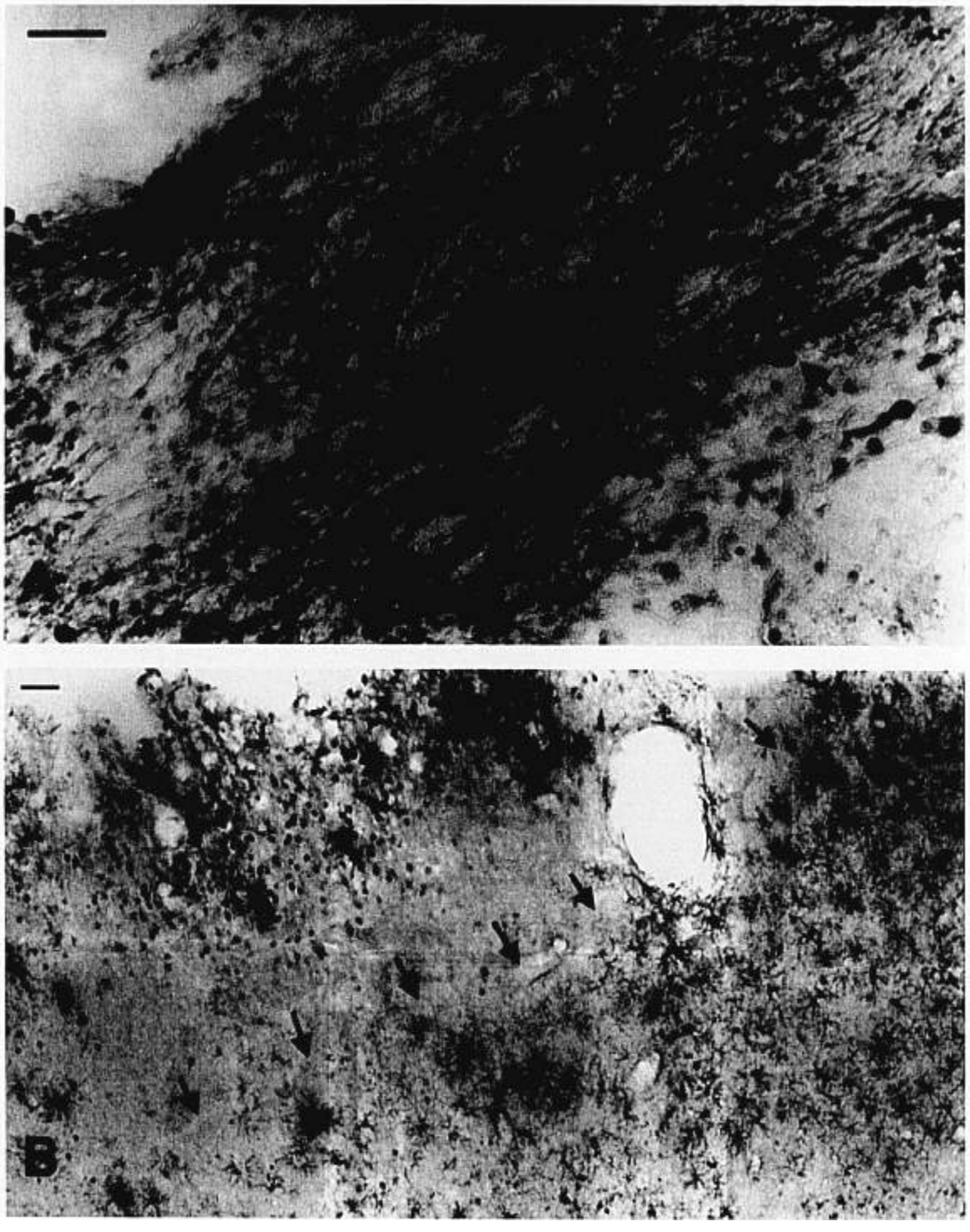

Fig. 8. Immunohistochemistry following high severity DCD. (A) Nonphosphorylated neurofilament protein (SMI 32) immunostained section ipsilateral to injury. Widespread terminal clubbing (arrows) was evident throughout the subcortical white matter bordering the injury site. No terminal clubbing was observed remote from the injury site. (B) Reactive astrocytosis was apparent in the ipsilateral cortex surrounding the injury site. In this case, a region virtually void of reactive astrocytes exists between the necrotic cavity and region of high immunoreactivity. Bars: 25 μm.

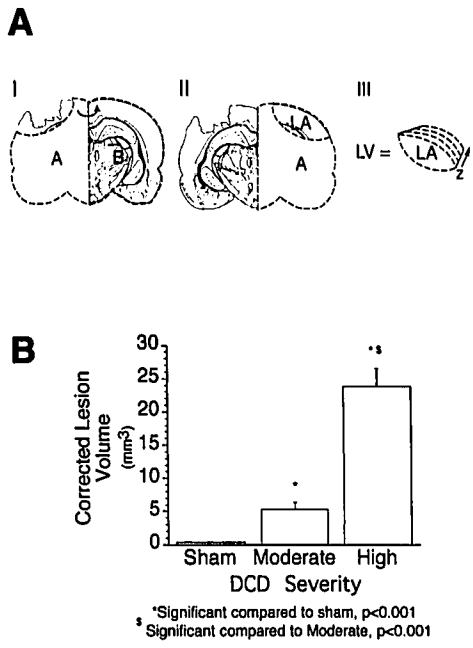

Fig. 9. Results of lesion volume analysis following experimental DCD (mean ± standard error). (A) Schematic overview of lesion volume analysis calculated from H&E sections. Using a pixel density threshold from an uninjured region, the lesion area was removed from the ipsilateral hemisphere (1). The remaining image was reflected and superimposed over the contralateral hemisphere image (2). The area difference between the 2 images was considered the corrected lesion area; the total lesion volume was calculated by summing the corrected lesion area across adjacent slices, multiplying by distance between sections (480 μm apart), and summing the product across rhe total lesion region. (B) An orthogonally designed ANOVA detected significant differences in lesion volume among the means for all groups, as well as between moderate and high severity groups ($p < 0.001$).

not correlate significantly to outcome following human head injury (32). Our data agrees with the clinical observations showing the release of glutamate from primary hemorrhage into the interstitial space was not sufficient to cause widespread injury. Rather, it may be glutamate release in combination with primary mechanical distortion and/or an ischemic insult that produces glutamate-mediated damage in vivo. Indeed, cultured neurons demonstrate a higher sensitivity to NMDA-induced calcium influx after a mechanical stretch (33), suggesting a possible relationship between tissue stretch and global changes in neurochemical levels. These interactions could be explored more in the future, and may identify mechanically induced changes in receptor structure and activation that are amenable to new therapeutic approaches for cell repair and recovery.

The findings presented in this report are a first step in better defining the histopathological and biomechanical differences between isolated focal contusions to the brain and more complex, multi-faceted injury pattern. Until now, it has been difficult to discern both the mechanistic and biomechanical overlap between these 2 injury patterns. We have shown that very focal deformation of the cortex produces only a contusion at the deformation site and no widespread damage. Therefore, we suggest that the widespread damage produced by other models of focal brain injury is due to the deformation of tissue, perhaps in combination with elevated neurochemical levels, and not solely the diffusion of potentially damaging substances from the injury site. Moreover, because our injury is well circumscribed and directly related to mechanical injury parameters, we anticipate that our data will yield an important mechanical criterion for injuring cortical tissue that is useful for predicting the conditions that cause these injuries in human. Thus, the dynamic cortical deformation method will help in defining both the mechanical and neurobiological sequelae of isolated cortical contusions.

ACKNOWLEDGMENTS

The authors gratefully acknowledge David I. Graham, MD, for his advice during the course of the studies and during the manuscript preparation. All animals procedures were approved by the University of Pennsylvania Institute for Animal Care and Use Committee. We adhered to the animal welfare guidelines set forth in the Guide for the Care and Use of Laboratory Animals, US Department of Health and Human Services Publication, 85-23.

REFERENCES

1. Adams JH, Graham DI. The pathology of blunt head injuries. In: Critchley M, O'Leary J, Jennet B, eds. Scientific Foundations of Neurology. Philadelphia: F.A. Davis Company, 1985
2. Adams JH, Graham DI, Scott G, Parker LS, Doyle D. Brain damage in fatal non-missile head injury. J Clin Pathol 1980;33:1132–45
3. Adams JH, Doyle D, Graham DI, et al. The contusion index: A reappraisal in human and experimental non-missile head injury. Neuropathol Appl Neurobiol 1985;11:299–308
4. Bullock R, Maxwell WL, Graham DI, Teasdale GM, Adams JH. Glial swelling following human cerebral contusion: An ultrastructural study. J Neurol Neurosurg Psychiatry 1991;54:427–34
5. Cervós-Navarro J, Lafuente JV. Traumatic brain injuries: Structural changes. J Neurol Sci 1991;102:S3–S14
6. Gennarelli TA. Animate models of human head injury [Review]. J Neurotrauma 1994;11:357–68
7. Smith D, Casey K, McIntosh T. Pharmacologic therapy for traumatic brain injury: Experimental approaches. New Horizons 1995; 3:562–72
8. McIntosh T, Smith D, Meaney D, Kotapka M, Gennarelli T, Graham D Neuropathological sequelae of traumatic brain injury: Relationship to neurochemical and biomechanical mechanisms [Review]. Lab Invest 1996;74:315–42
9. Mathew P, Graham DI, Bullock R, Maxwell W, McCulloch J, Teasdale G. Focal brain injury: Histological evidence of delayed inflammatory response in a new rodent model of focal cortical injury. Acta Neurochir (Wien) 1994;60S:428–30
10. Mathew P, Bullock R, Teasdale G, McCulloch J. Changes in local microvascular permeability and in the effect of intervention with 21-aminosteroid (tirilazad) in a new experimental model of focal cortical injury in the rat. J Neurotrauma 1996;13:465–72

11. McIntosh TK, Vink R, Noble L, et al. Traumatic brain injury in the rat: Characterization of a lateral fluid-percussion model. Neuroscience 1989;28:233–44
12. Goodman JC, Cherian L, Bryan RMJ, Robertson CS. Lateral cortical impact injury in rats: Pathologic effects of varying cortical compression and impact velocity. J Neurotrauma 1994;11:587–97
13. Adams JH, Scott G, Parker LS, Graham DI, Doyle D. The contusion index: A quantitative approach to cerebral contusions in head injury. Neuropathol Appl Neurobiol 1980;6:319–24
14. Gennarelli TA, Thibault LE. Biomechanics of head injury. In: Wilkins R, Rangachary SS, eds. Neurosurgery. New York: McGraw-Hill, 1985;1531–36
15. Ommaya AK, Thibault LE, Bandak FA. Mechanisms of impact head injury. International J Impact Engineering 1994;15:535–60
16. Ross DT, Graham DI, Adams JH, Gennarelli TA. Correlation of neurofilament immunohistochemistry with silver staining of damaged axons following head injury in humans, sub-human primates, and rodents. (Abstract). Soc. of Neuroscience Abstracts. 1992:1088
17. Ross DT, Meaney DF, Sabol MK, Smith DH, Gennarelli TA. Distribution of forebrain diffuse axonal injury following inertial closed head injury in miniature swine. Exp Neurol 1994;126:291–99
18. Pappius, HM, Brain injury: New insights into neurotransmitter and receptor mechanisms. Neurochem Research, 1991;16(9):941–49
19. Eacott, MJ, Heywood CA. Perception and memory: Action and interaction. Crit Rev Neurobiol, 1995;9(4):311–29
20. Kuroda Y, Fujisawa H, Strebel S, Graham DI, Bullock R. Effect of neuroprotective N-methyl-D-aspartate antagonists on increased intracranial pressure: studies in the rat acute subdural hematoma model. Neurosurgery 1994;35:106–12
21. Duhaime AC, Gennarelli LM, Yachnis A. Acute subdural hematoma: Is the blood itself toxic? J Neurotrauma 1994;11:669–78
22. Graham DI, Adams JH, Nicoll JA, Maxwell WL, Gennarelli TA. The nature, distribution, and causes of traumatic brain injury, Brain Pathol. 1995;5(4):397–406
23. Meaney DF, Ross DT, Winklestein BA, et al. Modification of cortical impact brain injury model to produce axonal damage in the rat cerebral cortex. J Neurotrauma 1994;11:599–612
24. Ueno K, Melvin JW, Li L, Lighthall JW. Development of tissue level brain injury criteria by finite element analysis. J Neurotrauma 1995;12:695–706
25. Thibault LE, Meaney DF, Anderson BJ, Marmarou A. Biomechanical aspects of a fluid percussion model of brain injury. J Neurotrauma 1992;9:311–22
26. Shreiber DI, McIntosh TK, Meaney DF. Focal damage to the blood-brain barrier induced by dynamic displacement of the cortex (abstract). J Neurotrauma 1996;13:595.
27. Mathew P, Bullock R, Graham DI, Maxwell WL, Teasdale GM, McCulloch J. A new experimental model of contusion in the rat. Histopathological analysis and temporal patterns of cerebral blood flow disturbances. J Neurosurg 1996;85:860–70
28. Galford JE, McElhaney JH. A viscoelastic study of scalp, brain, and dura. J Biomech 1970;3:211–21
29. Bullock R, Zauner A, Myseros JS, Marmarou A, Woodward JJ, Young HF. Evidence for prolonged release of excitatory amino acids in severe head trauma. Relationship to clinical events. Ann NY Acad Sci 1995;765:290–97
30. Baker CJ, Moulton RJ, Macmillan VH, Shedlen PM. Excitatory amino acids in cerebrospinal fluid following traumatic brain injury in humans. J Neurosurg 1993;79(3):369–72
31. Choi D, Malucci-Gedde M, Kriegstein AR. Glutamate toxicity in cortical cell culture. J Neurosci 1987;7:357–68
32. Brown J, Baker AJ, Konasiewicz SJ, Moulton RJ. Clinical significance of CSF glutamate concentrations following severe traumatic brain injury in humans. J Neurotrauma 1998;15(4):253–63
33. Zhang L, Rzigalinski BA, Ellis EF, Satin LS. Reduction of voltage-dependent Mg2+ blockade of NMDA current in mechanically injured neurons. Science 1996;274:1921–23

Received June 27, 1998
Revision received October 26, 1998
Accepted November 4, 1998